Group-Orthogonal Multicarrier CDMA

Xiaodong Cai, *Member, IEEE*, Shengli Zhou, *Member, IEEE*, and Georgios B. Giannakis, *Fellow, IEEE*

***Abstract*—In the presence of frequency-selective multipath fading channels, code-division multiple access (CDMA) suffers from multiuser interference (MUI) and intersymbol interference (ISI); but when properly designed, it enjoys multipath diversity. Orthogonal frequency-division multiple access (OFDMA) is MUI-free, but it does not enable the available channel diversity without employing error-control coding. On the other hand, coded OFDMA may achieve lower diversity than a CDMA system employing the same error-control codes. In this paper, we merge the advantages of OFDMA and CDMA to minimize MUI effects, and also enable the maximum available diversity for every user. In our group orthogonal multicarrier CDMA (GO-MC-CDMA) scheme, groups of users share a set of subcarriers. By judiciously choosing group subcarriers, we guarantee that every user transmits with maximum diversity. MUI is only present among users in the same group, and is suppressed via multiuser detection, which becomes practically feasible because we assign a small number of users per group. Performance is analyzed, and simulations are carried out to illustrate the merits of GO-MC-CDMA relative to existing alternatives.**

***Index Terms*—Diversity, fading channels, multicarrier code-division multiple access (MC-CDMA), multiuser detection (MUD).**

I. Introduction

In DIRECT-sequence code-division multiple access (DS-CDMA), each user's symbols are spread by a user-specific code, which expands the bandwidth compared with the data rate [18], [19], [23]. The wideband nature of DS-CDMA transmissions allows the receiver to resolve signals propagating through different paths, and gains multipath diversity to combat fading effects. While DS-CDMA spreads symbols in the time domain, multicarrier (MC)-CDMA introduces spreading in the frequency domain [9]. Although orthogonal CDMA user codes can be designed, the effective user codes, after the transmitted signal passes through a frequency-selective channel, are no longer orthogonal, which causes multiuser interference (MUI). While multiuser detection (MUD) can be used to mitigate the detrimental effects of MUI, MUD algorithms are relatively complex, and their implementation difficulty increases with the number of users [23]. This motivates well the design of MUI-free spreading codes for multiple access through frequency-selective fading channels.

Orthogonal frequency-division multiplexing (OFDM) leads to a promising MUI-free multiple-access technique that is termed orthogonal frequency-division multiple access (OFDMA) [20], where every user transmits on one or more subcarriers. Since subcarriers retain their orthogonality even after propagation through frequency-selective channels, MUI is eliminated by design. Unfortunately, OFDMA does not enable the multipath-induced diversity without employing error-control coding. On the other hand, for the same bandwidth, coded OFDMA may come with lower diversity than a coded CDMA system employing identical error-control codes. Generalized MC (GMC)-CDMA [25], which is a special case of a mutually orthogonal usercode receiver (AMOUR) system [4], transmits multiple symbols per user on a set of subcarriers using redundant linear precoding. GMC-CDMA not only eliminates MUI by design, but also enables multipath diversity without bandwidth overexpansion (see also [29]). Related schemes employing nonredundant linear precoding have been pursued for *single-user* transmissions over flat-fading channels [1], and frequency-selective channels [15], [27], [28] to enhance diversity and coding gain, to alleviate peak-to-average power effects [7], and recently, to improve performance of multiantenna systems [30]. While MUI is eliminated in GMC-CDMA, intersymbol interference (ISI) among each user's symbols always exists. Dynamic load changes in the system can be exploited to further improve the performance of GMC-CDMA in the low-load region, as discussed in [3] and [31]. The approaches in [3] and [31], however, need to change user code assignment and block length dynamically depending on the load, which may not be always feasible.

In order to exploit the maximum possible channel diversity while being able to accommodate dynamic load changes, we herein develop a group orthogonal (GO)-MC-CDMA scheme that does not require complex code assignment operations. We partition the set of subcarriers into groups; the users who are assigned subcarriers of the same group are separated via spreading codes. By judiciously grouping subcarriers, we guarantee that all the users achieve full multipath diversity. The users in each group are immune to interference from other groups, which explains why we name our scheme GO-MC-CDMA. Selecting groups of small size, we then apply MUD *per group*, which is practically feasible. In contrast, MUD for DS-CDMA or MC-CDMA needs to account for all active users, and thus has prohibitive complexity. A simple user allocation policy is exploited to accommodate dynamic load

Paper approved by V. A. Aalo, the Editor for Diversity and Fading Channel Theory of the IEEE Communications Society. Manuscript received April 19, 2002; revised February 23, 2003 and July 27, 2003. This work was prepared through collaborative participation in the Communications and Networks Consortium sponsored by the U. S. Army Research Laboratory under the Collaborative Technology Alliance Program, Cooperative Agreement DAAD19-01-2-0011. The U. S. Government is authorized to reproduce and distribute reprints for government purposes notwithstanding any copyright notation thereon. This paper was presented in part at the MILCOM Conference, Anaheim, CA, October 7–10, 2002.

X. Cai and G. B. Giannakis are with the Department of Electrical and Computer Engineering, University of Minnesota, Minneapolis, MN 55455 USA (e-mail: caixd@ece.umn.edu; georgios@ece.umn.edu).

S. Zhou is with the Department of Electrical and Computer Engineering, University of Connecticut, Storrs, CT 06269 USA (e-mail: shengli@engr.uconn.edu).

Digital Object Identifier 10.1109/TCOMM.2003.822174

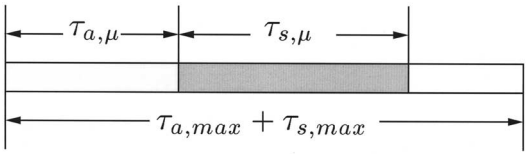

Fig. 1. Asynchronism and delay spread of user μ.

changes in the system, which enhances the error-probability performance at low load, as well as reducing the average complexity of MUD. User grouping for reducing MUI in MC systems with matched-filter reception was investigated in [5] and [6]. Striking tradeoffs among diversity, MUI, and receiver complexity, our work herein systematically develops a system enabling full multipath diversity, while affording low MUD-receiver complexity. Group MUD at the receiver without any MUI management at the transmitter was also pursued in [12] and [22].

The rest of the paper is organized as follows. We derive the GO-MC-CDMA system in Section II, and analyze its performance in Section III. In Section IV, GO-MC-CDMA and MC-CDMA are compared on the basis of complexity, and a MUI-free channel estimator is developed. Simulations are presented in Section V, and conclusions are drawn in Section VI.

Notation: Superscripts ^{T}, *, and $^{\mathcal{H}}$ denote transpose, conjugate, and Hermitian transpose, respectively. $E[\cdot]$ stands for expectation. Column vectors (matrices) are denoted by boldface lower- (upper-) case letters; $\mathbf{I}_N$ represents the $N \times N$ identity matrix; $\mathbf{1}_N$ denotes the $N \times 1$ vector with all one entries; $\boldsymbol{\mathcal{D}}(\mathbf{x})$ stands for a diagonal matrix with $\mathbf{x}$ on its diagonal; and $\|\mathbf{x}\|$ denotes the Euclidean norm of $\mathbf{x}$. The matrix $[\mathbf{F}_N]_{m,n} := N^{-1/2}\exp(-j2\pi(m-1)(n-1)/N)$ stands for the $N \times N$ fast Fourier transform (FFT) matrix. We will use Matlab's notation $\mathbf{A}(m:n,:)(\mathbf{A}(:,m:n))$ to extract the submatrix from row (column) m to row (column) n; $\mathbf{A}(m_1:m_2,n_1:n_2)$ to extract row m_1 to row m_2, and column n_1 to column n_2.

II. Design of GO-MC-CDMA

Our design targets the uplink of a quasi-synchronous system, where the mobile users have means of aligning their timing to a common reference time, as is the case, for example, in IS-95. The timing and delay spread of user μ are displayed in Fig. 1, where we denote by $\tau_{a,\mu}$ the asynchronism of user μ, and by $\tau_{s,\mu}$ the delay spread of user μ's channel. The maximum relative user asynchronism $\tau_{a,\max}$ arises between the nearest and the farthest mobiles, and is determined by the radius of the cell. The maximum delay spread $\tau_{s,\max}$ of the multipath channel in typical environments is often available by standard sounding techniques. Suppose that the system bandwidth is W, and let $T_c = 1/W$ denote the chip duration. After the propagation delay is taken into account, the chip-sampled discrete-time baseband-equivalent multipath channel (which also includes transmit–receive filters) of user μ can be modeled as a finite-impulse response (FIR) filter with delay T_c between consecutive taps. The total number of taps is $\lceil(\tau_{a,\max}+\tau_{s,\max})/T_c\rceil + 1$, [18, p. 797]. The channel impulse response (CIR) vector of user μ is written as $\mathbf{h}_\mu := [h_\mu(0), h_\mu(1), \ldots, h_\mu(L)]^T$, where $L = \lceil(\tau_{a,\max}+\tau_{s,\max})/T_c\rceil$ denotes the channel order. The first $L_{a,\mu} = \lfloor\tau_{a,\mu}/T_c\rfloor$ taps are zero; the next $L_{s,\mu} = \lceil(\tau_{a,\mu}+\tau_{s,\mu})/T_c\rceil - L_{a,\mu}$ taps are nonzero, while the last $L+1-L_{a,\mu}-L_{s,\mu}$ taps are zero. Note that $L_{s,\mu}$ is the channel delay spread of user μ, in terms of chip periods T_c. The maximum of $L_{s,\mu}$, $\forall\mu$, is denoted by $L_{s,\max}$. Since we will consider the uplink of a transmission system, we assume that: **AS1**) the channels of different users are statistically independent.

A. User Grouping

We first consider the symbol-spread case, where each active user transmits only one symbol over a block of M chips. Let the symbol period be $T = MT_c$. The entire available bandwidth is utilized with M subcarriers that are spaced $1/T$ apart from each other. If $\mathbf{f}_i$ denotes the ith column of the FFT matrix $\mathbf{F}_M$, then $\mathbf{f}_i^*$ is the ith digital subcarrier. We partition the M subcarriers into N_g groups with each group having $Q = M/N_g$ subcarriers. Since both M and N_g are design parameters, we can properly choose M and N_g, so that Q is an integer satisfying $Q \geq L_{s,\max}$. A user chooses a specific group of subcarriers to transmit its information-bearing symbols; and Q users share Q subcarriers per group, which ensures no spectral efficiency loss.

The system model of GO-MC-CDMA is illustrated in the block diagram of Fig. 2. Let $s_{n,m}(i)$ be the information-bearing symbol of user m in the nth group transmitted during the time interval $[iT,(i+1))T$. A $Q \times 1$ spreading code $\mathbf{c}_m$ is used to spread $s_{n,m}(i)$ to the Q subcarriers of the nth group. Define the $Q \times Q$ matrix $\mathbf{C} := [\mathbf{c}_0, \mathbf{c}_1, \ldots, \mathbf{c}_{Q-1}]$, whose columns consist of Q spreading codes of the nth group. The spreading code matrix $\mathbf{C}$ does not have to be identical for different groups. But since there is no MUI between users of different groups by design, we choose the same code matrix for all the groups. We further design $\mathbf{C}$ so that we have the following.

C1) All user codes are linearly independent, with $|c_q(i)|^2 = 1/Q$, $\forall q, i = 1, \ldots, Q$, where $c_q(i)$ is the ith entry of $\mathbf{c}_q$.

This design condition is satisfied when $\mathbf{c}_q$ is a scaled binary code, e.g., Walsh–Hadamard or Gold [18]; or any constant modulus complex-field code from ones in [30]. Let the columns of the $M \times Q$ matrix $\mathbf{F}_n^*$ comprise the Q digital subcarriers of the nth group. While any Q subcarriers can be assigned to a group of users, we select a set of equispaced subcarriers, which results in the following matrix:

$$\mathbf{F}_n^* = \left[\mathbf{f}_n^*, \mathbf{f}_{Ng+n}^*, \mathbf{f}_{2Ng+n}^*, \ldots \mathbf{f}_{(Q-1)N_g+n}^*\right]. \quad (1)$$

This group subcarrier assignment is illustrated in Fig. 3, using $M = 9$, $N_g = 3$, and $Q = 3$. It will turn out that this equispaced group subcarrier assignment, along with condition C1) on the spreading codes, is optimal in the sense that the minimum error probability is achieved, when there is only one active user in a group. The $M \times 1$ signal vector of user m in the nth group during the ith block, modulated on Q subcarriers, can be expressed as

$$\mathbf{x}_{n,m}(i) = \mathbf{F}_n^* \mathbf{c}_m s_{n,m}(i). \quad (2)$$

After parallel-to-serial (P/S) conversion, a cyclic prefix (CP) of length L chips is added to each block, and the signal is transmitted over a frequency-selective fading channel. Since the sub-

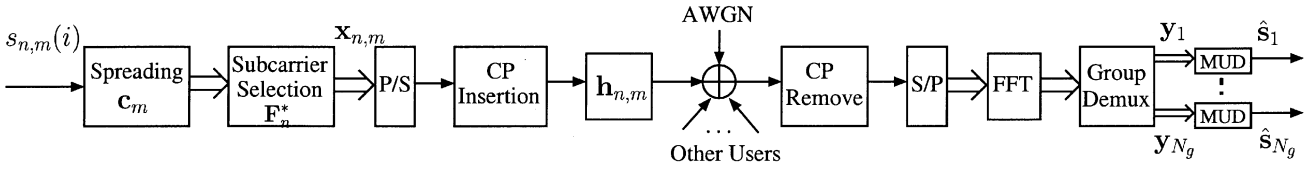

Fig. 2. System model.

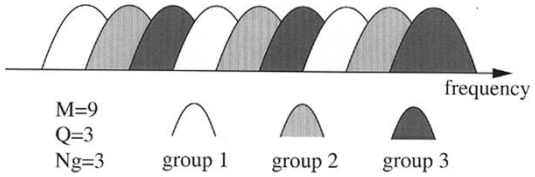

Fig. 3. Equispaced group subcarrier assignment.

carriers in a group are equispaced, the matrix $\mathbf{F}_n^*$ in (1) can also be written as

$$\mathbf{F}_n^* = \mathbf{D}_n \left(\mathbf{1}_{N_g} \otimes \mathbf{F}_Q^{\mathcal{H}}\right) \tag{3}$$

where $\mathbf{D}_n := \mathrm{diag}(1, \exp(j2\pi n/M), \ldots, \exp(j2\pi n(M-1)/M)$, and $\otimes$ represents the Kronecker product. Notice that $\mathbf{x}_{n,m}(i)$ in (2) can be computed using a Q-point FFT, and $M+1$ complex multiplications, which considerably reduces complexity (especially with M large) when compared with the case where Q subcarriers in a group are arbitrarily chosen.

At the receiver end, after removing the CP to eliminate interblock interference (IBI), and FFT processing the IBI-free signal, we demultiplex the received samples belonging to different groups of subcarriers. Let $\bar{\mathbf{h}}_{n,m} := [H_{n,m}(e^{-j2\pi n/M}), \ldots, H_{n,m}(e^{-j2\pi(n+(Q-1)N_g)/M})]$ contain the frequency response samples on the FFT grid of the FIR channel of the mth user in the nth group. The $Q \times 1$ data vector for the nth group can be written as [25]

$$\begin{aligned} \mathbf{y}_n &= \sum_{m=0}^{N_{a,n}-1} \mathbf{D}(\bar{\mathbf{h}}_{n,m})\mathbf{c}_m s_{n,m} + \mathbf{w}_n \\ &= \sum_{m=0}^{N_{a,n}-1} \mathbf{D}(\mathbf{c}_m)\bar{\mathbf{h}}_{n,m} s_{n,m} + \mathbf{w}_n \end{aligned} \tag{4}$$

where $N_{a,n}$ is the number of active users in the nth group, and $\mathbf{w}_n$ is zero-mean complex additive white Gaussian noise (AWGN) with variance $N_0/2$ per dimension. Since there is no IBI, we have dropped the block index i for notational simplicity. Let $\tilde{\mathbf{c}}_{n,m} := \boldsymbol{\mathcal{D}}(\mathbf{c}_m)\bar{\mathbf{h}}_{n,m}$ denote the effective spreading code of user m, and define $\tilde{\mathbf{C}}_n := [\tilde{\mathbf{c}}_{n,0}, \ldots, \tilde{\mathbf{c}}_{n,Na,n-1}]$, and $\mathbf{s}_n := [s_{n,0,\ldots,s_{n,Na,n-1}}]^T$. Then $\mathbf{y}_n$ in (4) can be written as

$$\mathbf{y}_n = \tilde{\mathbf{C}}_n \mathbf{s}_n + \mathbf{w}_n. \tag{5}$$

Based on $\mathbf{y}_n$ in (4) or (5), MUD can be applied to detect the information-bearing symbols $\{s_{n,m}\}_{m=0}^{N_{a,n}-1}$ in the nth group.

In order to reduce the loss of bandwidth and power efficiency due to CP, as well as accommodate users with different quality of service (QoS), we incorporate the *block spreading* approach [4], [25], [26], where $K > 1$ symbols are transmitted per user per block. We have KM subcarriers to transmit a total of KM symbols per block without increasing signal bandwidth. Now, let us partition the subcarriers into $N_g = KM/Q$ groups. Each user is assigned to K groups, and transmits one symbol in each group. At the receiver, using the K input–output equations (4), we detect K symbols of the same user independently. This block spreading of GO-MC-CDMA avoids ISI among symbols from the same user, which facilitates accommodation of the dynamic load changes in the system to improve the performance at low load; whereas, the block spreading of GMC-CDMA in [4] and [25] eliminates MUI, but ISI always exists no matter how the system load changes. Actually, it is possible to combine GO-MC-CDMA with GMC-CDMA to design a hybrid block spreading system, where users with identical QoS can rely on block spreading of GO-MC-CDMA, while other users can employ the block spreading of GMC-CDMA to isolate themselves from other users. In other words, we have a lot of flexibility in configuring the system, trading off MUI for ISI, and even accommodate different symbol rates as suggested in [26].

B. User Allocation

Dynamic subcarrier assignment is employed in [3] and [31] to improve the performance when the system load is low. In GO-MC-CDMA, the base station allocates active users uniformly to different groups. For M_a active users in the system, let $\tilde{N}_a := \lfloor M_a/N_g \rfloor$, and $N_{g1} := M_a - N_g\tilde{N}_a - 1$; then, the number of active users allocated to the nth group is

$$N_{a,n} = \begin{cases} \tilde{N}_a + 1, & n = 0, \ldots, N_{g1} \\ \tilde{N}_a, & n = N_{g1}+1, \ldots, N_g - 1. \end{cases} \tag{6}$$

When a new user arrives, it is assigned to group $N_{g1}+1$. If $M_a \leq N_g$, every active user enjoys single-user performance, because it is the only active user in its group. Since the performance of a user and the computational complexity of maximum-likelihood (ML) detection depends on the number of active users in a group, this simple user-allocation policy enhances the performance, while at the same time, reduces average computational complexity.

Remark 1: In MC-CDMA [9], [10], all users share the signal bandwidth, which renders optimal MUD computationally prohibitive as the number of active users increases. In our GO-MC-CDMA design, a small group of users shares a set of subcarriers. Actually, it will be shown in the next section that the group size only needs to be $\geq L_{s,\max}$ to enable maximum diversity per user. For such sizes, the optimal MUD becomes practically feasible.

III. Performance Analysis

Define a $Q \times L_{s,n,m}$ matrix $\mathbf{F}_{n,m} := \sqrt{M}\mathbf{F}_n^T(:, L_{a,n,m}+1 : L_{a,n,m}+L_{s,n,m})$, where $L_{a,n,m}$ and $L_{s,n,m}$ account, respectively, for the asynchronism and the delay spread of the mth user in the nth group, as discussed in Section II. From (3), we see that any Q consecutive rows of $\mathbf{F}_n$ are orthogonal; and since $Q \geq L_{s,n,m}$, it is easy to verify that

$$\mathbf{F}_{n,m}^{\mathcal{H}}\mathbf{F}_{n,m} = Q\mathbf{I}_{L_{s,n,m}}. \tag{7}$$

Let vector $\mathbf{h}_{n,m}$ contain the $L_{s,n,m}$ taps of the CIR of user m in the nth group. Then, the channel frequency response vector $\bar{\mathbf{h}}_{n,m}$ in (4) can be expressed as $\bar{\mathbf{h}}_{n,m} = \mathbf{F}_{n,m}\mathbf{h}_{n,m}$.

A. Single-User Performance

Suppose that only user 0 is active in the nth group. The received signal vector of the nth group is then simplified from (4) to

$$\mathbf{y}_n = \mathbf{D}(\mathbf{c}_0)\bar{\mathbf{h}}_{n,0}s_0 + \mathbf{w}_n. \tag{8}$$

The optimal single-user receiver is the matched filter. The decision variable, obtained from the output of the matched filter, is given by $z = \bar{\mathbf{h}}_{n,0}^H\boldsymbol{\mathcal{D}}(\mathbf{c}_0^*)\mathbf{y}_n = \mathbf{h}_{n,0}^{\mathcal{H}}\mathbf{F}_{n,0}^{\mathcal{H}}\boldsymbol{\mathcal{D}}(\mathbf{c}_0^*)\mathbf{y}_n$. Under the constant modulus condition C1), and using (7), we have $\mathbf{F}_{n,0}^{\mathcal{H}}\boldsymbol{\mathcal{D}}(\mathbf{c}_0^*)\boldsymbol{\mathcal{D}}(\mathbf{c}_0)\mathbf{F}_{n,0} = \mathbf{I}_{L_{s,n,0}}$; and the decision variable becomes

$$z = \|\mathbf{h}_{n,0}\|^2 s_0 + \eta \tag{9}$$

where η is a Gaussian random variable with variance $\|\mathbf{h}_{n,0}\|^2 N_0$. The signal-to-noise ratio (SNR) of z in (9) is $|s_0|^2\|\mathbf{h}_{n,0}\|^2/N_0$. It is seen from (9) that the decision variable z optimally combines the transmitted symbol s_0 from all the paths, similar to a maximum ratio combiner, which maximizes the SNR, and thereby minimizes error probability. Note that this performance is better than the matched-filter bound of single-carrier transmissions and the single-user performance of DS-CDMA, since in either case, self-interference is present from different paths. From this analysis, we see that the equispaced group subcarrier assignment, along with the constant modulus condition in C1), guarantees the optimal single-user performance. Without these two conditions, the SNR of the decision variable z may not be maximized. In summary, we have established the following lemma.

Lemma 1: If there is only one active user in a group, and the delay spread of its multipath channel has order L_s, then under condition C1), minimum error probability performance is achieved by transmitting a symbol on $Q > L_s$ equispaced subcarriers.

This single-user performance analysis reveals that a user does not need to transmit over the entire bandwidth to achieve maximum diversity, which makes it possible to *reduce MUI without sacrificing diversity*. This observation should not be surprising, because it is well known that frequency diversity can be obtained by transmitting on carrier frequencies which are separated from each other by the channel's coherence bandwidth. However, together with the equispaced subcarrier grouping we adopted, it provides within the MC-CDMA framework a means of achieving maximum diversity with as few interfering users as possible.

B. Multiuser Performance

Consider the received signal of the nth group given in (4) or (5). For notational brevity, we will henceforth omit the group index n in $N_{a,n}$, $\mathbf{s}_n$, $\tilde{\mathbf{C}}_n$, and $L_{s,n,m}$. Since the size of each group is small, an ML receiver can be employed to jointly detect the symbols of all active users in each group. To analyze the ML performance, we will derive the union bound on symbol-error rate (SER). Suppose that we are interested in the SER of user 0 in the nth group. The symbol vector in (5) can be written as $\mathbf{s} := [s_0\ \mathbf{s}_I^T]^T$, where s_0 is the symbol of user 0, and $\mathbf{s}_I$ contains other active users' symbols. Let $\tilde{\mathbf{s}} := [\tilde{s}_0\ \tilde{\mathbf{s}}_I^T]^T$ be a symbol vector such that $\tilde{s}_0 \neq s_0$, and let $\mathbf{h}$ comprise the CIRs of all active users in the nth group; i.e., $\mathbf{h} := [\mathbf{h}_{n,0}^T, \mathbf{h}_{n,1}^T, \ldots, \mathbf{h}_{n,N_a-1}^T]^T$. Define the conditional pairwise error probability (PEP), $P(\mathbf{s} \to \tilde{\mathbf{s}}|\mathbf{h})$, as the probability that the detector decides in favor of $\tilde{\mathbf{s}}$, when $\mathbf{s}$ is actually transmitted, given the channel realization $\mathbf{h}$. The conditional PEP can be upper bounded using the Chernoff bound as [18, p. 55]

$$P(\mathbf{s} \to \tilde{\mathbf{s}}|\mathbf{h}) \leq \exp\left(-\frac{\left\|\tilde{\mathbf{C}}(\tilde{\mathbf{s}}-\mathbf{s})\right\|^2}{4N_0}\right). \tag{10}$$

Let the error vector $\mathbf{e} := \tilde{\mathbf{s}} - \mathbf{s} = [e_0, e_1, \ldots, e_{N_a-1}]^T$, and define $\mathbf{S}_{e,m} := e_m\boldsymbol{\mathcal{D}}(\mathbf{c}_m)\mathbf{F}_{n,m}$, and $\mathbf{S}_e := [\mathbf{S}_{e,0}, \mathbf{S}_{e,1}, \ldots, \mathbf{S}_{e,N_a-1}]$. Then, we have $d^2 := \|\tilde{\mathbf{C}}(\tilde{\mathbf{s}} - \mathbf{s})\|^2 = \|\sum_{m=0}^{N_a-1}\mathbf{S}_{e,m}\mathbf{h}_{n,m}\|^2 = \mathbf{h}^{\mathcal{H}}\mathbf{S}_e^{\mathcal{H}}\mathbf{S}_e\mathbf{h}$. Letting $\mathbf{R}_m := E[\mathbf{h}_{n,m}\mathbf{h}_{n,m}^{\mathcal{H}}]$, we obtain $\mathbf{R} := E[\mathbf{h}\mathbf{h}^{\mathcal{H}}] = \mathrm{diag}(\mathbf{R}_0, \ldots, \mathbf{R}_{N_a-1})$, since different users' channels are independent. The unconditional PEP, $P(\mathbf{s} \to \tilde{\mathbf{s}})$, can be found by averaging $P(\mathbf{s} \to \tilde{\mathbf{s}}|\mathbf{h})$ over all realizations of $\mathbf{h}$. Since d^2 is a quadratic form of the complex Gaussian random vector $\mathbf{h}$, we can use the characteristic function of d^2 given in [21, p. 595] to derive the following upper bound of $P(\mathbf{s} \to \tilde{\mathbf{s}})$ from (10):

$$P(\mathbf{s} \to \tilde{\mathbf{s}}) < \left|\mathbf{I} + \frac{\mathbf{S}_e^{\mathcal{H}}\mathbf{S}_e\mathbf{R}}{4N_0}\right|^{-1}. \tag{11}$$

The SER of user 0, $P(e)$, is upper bounded by the union bound as follows:

$$P(e) < \sum_{\mathbf{s}}\sum_{\tilde{\mathbf{s}}} P(\mathbf{s})P(\mathbf{s} \to \tilde{\mathbf{s}}) \tag{12}$$

where $P(\mathbf{s})$ is the probability of the transmitting symbol vector $\mathbf{s}$. Let $\mathcal{A}$ denote the alphabet (constellation) from which users' symbols are drawn, and let $|\mathcal{A}|$ be the cardinality of $\mathcal{A}$. Assuming that all symbols in $\mathcal{A}$ are taken with equal probability, and all users' symbols are independent, it follows that $P(\mathbf{s}) = |\mathcal{A}|^{-N_a}$. While we are now ready to evaluate the union bound on SER by substituting (11) into (12), we will pursue more insightful bounds.

Since the correlation matrix $\mathbf{R}_m$ is positive semidefinite, we can use Cholesky's decomposition to find a matrix $\mathbf{R}_m^{1/2}$ such that $\mathbf{R}_m = \mathbf{R}_m^{1/2}(\mathbf{R}_m^{1/2})^{\mathcal{H}}$. Defining

$\mathbf{R}^{1/2} := \text{diag}(\mathbf{R}_0^{1/2}, \ldots, \mathbf{R}_{N_a-1}^{1/2})$ and $\mathbf{A} := \mathbf{S}_e\mathbf{R}^{1/2}$, and using the identity $|\mathbf{I}+\mathbf{XY}| = |\mathbf{I}+\mathbf{YX}|$, we can write (11) as

$$P(\mathbf{s} \to \tilde{\mathbf{s}}) < \left|\mathbf{I} + \frac{\mathbf{A}\mathbf{A}^{\mathcal{H}}}{4N_0}\right|^{-1}. \tag{13}$$

To derive our PEP bound, we need [11, Corollary 4.3.3, p. 182], which we state here with slightly modified notation.

Lemma 2 [11]: Suppose that the $N \times N$ Hermitian matrices $\mathbf{X}$ and $\mathbf{Y}$ are positive semidefinite, and let $\{\lambda_{X,i}\}_{i=1}^{N}$ denote the eigenvalues of $\mathbf{X}$ arranged in nonincreasing order. If $\mathbf{Z} = \mathbf{X}+\mathbf{Y}$, and $\{\lambda_{Z,i}\}_{i=1}^{N}$ are the eigenvalues of $\mathbf{Z}$ in nonincreasing order, then we have $\lambda_{Z,i} \geq \lambda_{X,i}, \forall i$.

Note that *Lemma 2* also guarantees that rank $(\mathbf{Z}) \geq$ rank $(\mathbf{X})$. From the definition of $\mathbf{A}$, we have

$$\mathbf{A}\mathbf{A}^{\mathcal{H}} = \sum_{i=0}^{N_a-1} \mathbf{S}_{e,i}\mathbf{R}_i\mathbf{S}_{e,i}^{\mathcal{H}}. \tag{14}$$

Let $r_i :=$ rank $(\mathbf{R}_i)$, and $\{\kappa_{i,j}\}_{j=1}^{r_j}$ denote the nonzero eigenvalues of $\mathbf{R}_i$ in nonincreasing order. Since $\mathbf{S}_{e,i}\mathbf{R}_i\mathbf{S}_{e,i}^{\mathcal{H}}$ and $(\mathbf{R}_i^{1/2})^{\mathcal{H}}\mathbf{S}_{e,i}^{\mathcal{H}}\mathbf{S}_{e,i}\mathbf{R}_i^{1/2} = |e_i|^2(\mathbf{R}_i^{1/2})^{\mathcal{H}}\mathbf{R}_i^{1/2}$ share the same nonzero eigenvalues, and $(\mathbf{R}_i^{1/2})^{\mathcal{H}}\mathbf{R}_i^{1/2}$ has the same set of nonzero eigenvalues as $\mathbf{R}_i$, the nonzero eigenvalues of $\mathbf{S}_{e,i}\mathbf{R}_i\mathbf{S}_{e,i}^{\mathcal{H}}$ are $\{|e_i|^2\kappa_{i,j}\}_{j=1}^{r_j}$, if $e_i \neq 0$. Let $r_A :=$ rank $(\mathbf{A})$ and $\{\lambda_i\})_{i=1}^{r_A}$ denote the nonzero eigenvalues of $\mathbf{A}\mathbf{A}^{\mathcal{H}}$ in nonincreasing order. Since $\mathbf{S}_{e,i}\mathbf{R}_i\mathbf{S}_{e,i}^{\mathcal{H}}$ is positive semidefinite, $\forall i$, from (14) and *Lemma 2*, we have $\lambda_j > |e_i|^2\kappa_{i,j}, j = 1, \ldots, r_i$. Using the identity $|\mathbf{I}+\mathbf{A}\mathbf{A}^{\mathcal{H}}/(4N_0)| = \prod_{j=1}^{r_A}[1+\lambda_j/(4N_0)]$, we obtain

$$\begin{aligned}\left|\mathbf{I} + \frac{\mathbf{A}\mathbf{A}^{\mathcal{H}}}{4N_0}\right| &> \prod_{j=1}^{r_i}\left(1+\frac{|e_i|^2\kappa_{i,j}}{4N_0}\right)\prod_{j=r_i+1}^{r_A}\left(1+\frac{\lambda_j}{4N_0}\right) \\ &= \left|\mathbf{I}+\frac{|e_i|^2\mathbf{R}_i}{4N_0}\right|\prod_{j=r_i+1}^{r_A}\left(1+\frac{\lambda_j}{4N_0}\right), \quad \forall i \end{aligned} \tag{15}$$

where *Lemma 2* guarantees $r_A \geq r_i$. Letting $\tilde{r}$ be the rank of $\mathbf{R}_i$ that maximizes $|\mathbf{I} + |e_i|^2\mathbf{R}_i/(4N_0)|$, and combining (13) and (15), we obtain the following upper bound on PEP:

$$P(\mathbf{s} \to \tilde{\mathbf{s}}) < \left[\max_i\left(\left|\mathbf{I}+\frac{|e_i|^2\mathbf{R}_i}{4N_0}\right|\right)\prod_{j=\tilde{r}+1}^{r_A}\left(1+\frac{\lambda_j}{4N_0}\right)\right]^{-1}. \tag{16}$$

Define two subsets of the vector $\tilde{\mathbf{s}}$: $\tilde{\mathcal{S}}_1 := \{\tilde{\mathbf{s}} : \tilde{s}_0 \neq s_0, \tilde{\mathbf{s}}_I = \mathbf{s}_I\}$, and $\tilde{\mathcal{S}}_2 := \{\tilde{\mathbf{s}} : \tilde{s}_0 \neq s_0, \tilde{\mathbf{s}}_I \neq \mathbf{s}_I\}$; and let $\tilde{\mathbf{s}}_1 \in \tilde{\mathcal{S}}_1$, and $\tilde{\mathbf{s}}_2 \in \tilde{\mathcal{S}}_2$. From (16), we see that the diversity order of the single-error PEP, $P(\mathbf{s} \to \tilde{\mathbf{s}}_1)$, is the rank of $\mathbf{R}_0$, and the multiple error PEP, $P(\mathbf{s} \to \tilde{\mathbf{s}}_2)$, has a diversity order equal to, or greater than, that of the single-error PEP. Thus, we have established the following result.

Proposition 1: Under AS1), every GO-MC-CDMA user enables the maximum diversity order by using equispaced group subcarriers and a spreading code satisfying C1). The maximum achievable diversity order per user is the rank of the correlation matrix of the corresponding frequency-selective channel.

Proposition 1 confirms that we have accomplished one of our major goals in designing GO-MC-CDMA: to enable maximum diversity for every user.

From (16), we see that the multiple-error PEP is always less than the bound on single-error PEP, which reveals that strong users do not degrade the performance of other relatively weak users across the SNR region. We can also express the union bound in (12) as

$$P(e) < |\mathcal{A}|^{-N_a}\sum_{\mathbf{s}}\left[\sum_{\tilde{\mathbf{s}}_1}P(\mathbf{s} \to \tilde{\mathbf{s}}_1) + \sum_{\tilde{\mathbf{s}}_2}P(\mathbf{s} \to \tilde{\mathbf{s}}_2)\right]. \tag{17}$$

Define the union bound on single-error PEP as $P_1(e) := |\mathcal{A}|^{-N_a}\sum_{\mathbf{s}}\sum_{\tilde{\mathbf{s}}_1}P(\mathbf{s} \to \tilde{\mathbf{s}}_1)$. Since the size of the set $\tilde{\mathcal{S}}_2$ is $|\mathcal{A}|^{N_a-1}$ with $N_a \leq Q$, which is small by design, we deduce from (16) and (17) that the union bound on SER in a multiuser environment is close to $P_1(e)$ at high SNR, which implies that multiuser SER approaches single-user SER. This will be corroborated by the numerical results and simulations of Section V.

IV. Receiver Complexity and Channel Estimation

Since there is no MUI among users in different groups, the receiver only needs to jointly detect the information-bearing symbols from the users in the same group. The group size Q is up to the designer. In order for the optimal MUD to be computationally feasible, the group size should be chosen as small as possible under the constraint that the channel diversity can be ensured fully, or approximately so. The diversity order provided by a multipath channel is determined by the wireless environment and the bandwidth of the transmitted signal. How much diversity will be collected certainly also depends on the receiver. For example, in a typical urban environment, RAKE reception in the IS-95 CDMA system can resolve three to five paths. When the signal bandwidth increases, more paths can be resolved to enhance diversity. However, given an uncoded bit-error rate (BER) level, increasing the diversity order beyond a certain level may not result in significant performance gain. For instance, when the uncoded BER is targeted to be 10^{-4} for binary phase-shift keying (BPSK), the performance gain brought by every diversity order beyond six is negligible in the practical SNR range. Therefore, in most cases, we can choose $Q \leq 6$. For groups of such a small size, ML detection becomes feasible, since there are only $N_a \leq Q$ active users per group. In this section, we will compare the receiver complexity of GO-MC-CDMA and MC-CDMA. GMC-CDMA with load adaptation employs dynamic subcarrier assignment, which is a medium access control (MAC) layer operation, and also increases the transmitter complexity. Hence, we will not compare the receiver complexity of GMC-CDMA with that of GO-MC-CDMA. Since channel state information (CSI) is required at the receiver, we will also develop a channel estimation scheme.

A. Receiver Complexity

For the input–output relation (5), the ML detector is

$$\begin{aligned}\hat{\mathbf{s}} &= \arg\min_{\mathbf{s}\in\mathcal{A}^{N_a}}\|\mathbf{y}_n - \tilde{\mathbf{C}}_n\mathbf{s}\|^2 \\ &= \arg\min_{\mathbf{s}\in\mathcal{A}^{N_a}}\left[-2\Re(\mathbf{s}^{\mathcal{H}}\tilde{\mathbf{C}}_n^{\mathcal{H}}\mathbf{y}_n) + \mathbf{s}^{\mathcal{H}}\tilde{\mathbf{C}}_n^{\mathcal{H}}\tilde{\mathbf{C}}_n\mathbf{s}\right]. \end{aligned} \tag{18}$$

Note that when the total number of active users is less than or equal to the number of groups, i.e., $M_a \leq N_g$, then

each group contains, at most, one user, and the ML detector is simply a matched filter. Define a flop as a complex floating point operation [8, p. 18]. Calculating $\tilde{\mathbf{C}}_n^{\mathcal{H}}\tilde{\mathbf{C}}_n$ and $\tilde{\mathbf{C}}_n^{\mathcal{H}}\mathbf{y}_n$ requires $2N_a^2Q$ and $2N_aQ$ flops, respectively; while $f(N_a,Q) := |\mathcal{A}|^{N_a}(2N_a^2+5N_a)+2N_a^2Q+2N_aQ$ flops are required to search over all the possible sequences $\mathbf{s}$. Then, with the uniform user allocation in (6), the average number of flops per user required by the ML detector is

$$N_{fp,\mathrm{GO}} = \begin{cases} 2Q, & M_a \le N_g \\ \frac{\{2Q(N_g-N_{g1})+N_{g1}f(2,Q)\}}{M_a}, & N_g < M_a \le 2N_g \\ \frac{\{(N_g-N_{g1})f(\tilde{N}_a,Q)+N_{g1}f(\tilde{N}_a+1,Q)\}}{M_a}, & M_a > 2N_g. \end{cases} \tag{19}$$

Note that the complexity for ML detection in GO-MC-CDMA increases exponentially with the number of *active users per group*, but not with the total number of active users in the system.

Let us now consider the receiver complexity of MC-CDMA. When the ML detector is employed, the average number of flops per user is given by

$$N_{fp,\mathrm{MC1}} = \begin{cases} 2M, & M_a = 1 \\ f(M_a,M), & M_a > 1. \end{cases} \tag{20}$$

The computation of the ML detector increases exponentially with the total number of active users in the system. Because of the prohibitive complexity of ML detection even with a moderate number of active users, we may consider utilizing a linear minimum mean-square error (MMSE) detector for MC-CDMA. Let us consider the MMSE detector for the block $\mathbf{s}$ in (5). The MMSE detector is given by $\mathbf{G} = \tilde{\mathbf{C}}_n^{\mathcal{H}}\mathbf{R}_y^{-1}$, where $\mathbf{R}_y = \tilde{\mathbf{C}}_n\tilde{\mathbf{C}}_n^{\mathcal{H}} + N_0\mathbf{I}_Q$. Alternatively, the MMSE detector can be found as $\tilde{\mathbf{G}} = \tilde{\mathbf{R}}_y^{-1}\tilde{\mathbf{C}}_n^{\mathcal{H}}$ [23], where $\tilde{\mathbf{R}}_y = \tilde{\mathbf{C}}_n^{\mathcal{H}}\tilde{\mathbf{C}}_n + N_0\mathbf{I}_{N_a}$. It can be shown that these two MMSE detectors lead to the same MSE. However, the MMSE detector $\tilde{\mathbf{G}}$ requires fewer computations because it inverts the $N_a \times N_a$ matrix $\tilde{\mathbf{R}}_y$. The major computational burden in the MMSE detector is computing and inverting the covariance matrix $\tilde{\mathbf{R}}_y$. By using Gaussian elimination, inverting an $N_a \times N_a$ matrix needs $2N_a^3/3$ flops [8, p. 112]. Since the signal model of MC-CDMA is in the same form as (5), except that Q and N_a are replaced by M and M_a, the average number of flops per user for the MMSE detector in MC-CDMA is found to be

$$N_{fp,\mathrm{MC2}} = \frac{2M_a^2}{3} + 2M_aM + 2M + 2M_a + 1. \tag{21}$$

We plot $N_{fp,\mathrm{GO}}$, $N_{fp,\mathrm{MC1}}$, and $N_{fp,\mathrm{MC2}}$ in Fig. 4 with $|\mathcal{A}| = 4$, $M = 64$, and $Q = 4$. It is seen that in this case, the ML detector of GO-MC-CDMA has lower complexity than the MMSE detector of MC-CDMA, even when the load is full. The complexity of MMSE detection in MC-CDMA depends on the processing gain M. With a typical value $M = 64$, which is identical to the processing gain in IS-95, the MMSE detector still requires large computation. On the other hand, the maximum complexity of ML detection in GO-MC-CDMA is determined by the group size Q, and the constellation size $|\mathcal{A}|$. As we discussed, Q can be chosen to be less than seven for most practical cases. If the constellation size is large, we can use an approximate ML detector that relies on the sphere decoding algorithm, whose complexity is approximately on the order of $\mathcal{O}(N_a^3)$, regardless of the constellation [24]. Furthermore, GO-MC-CDMA employs N_g ML detectors for the N_g groups. This parallel structure can be efficiently implemented in hardware. In short, the complexity of the ML detector for GO-MC-CDMA is affordable; it is lower than that of linear MMSE detection for MC-CDMA with a typical processing gain.

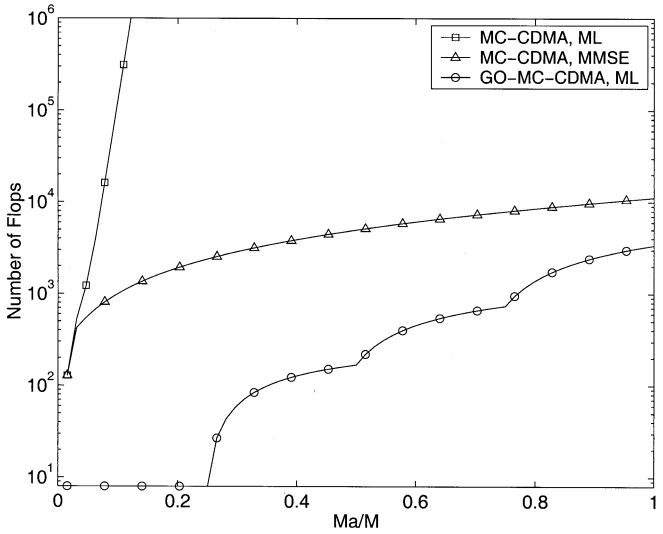

Fig. 4. Average number of flops per user: $|\mathcal{A}| = 4$, $M = 64$, and $Q = 4$.

B. Channel Estimation

Both the ML and the MMSE detectors require CSI of all active users in a group. In uplink, the CIRs of different users are different, which makes channel estimation more challenging than the downlink. We can multiplex a user's pilot symbols with the information-bearing symbols to enable channel estimation at the receiver [2], [14]. However, since the length of the user codes (columns of matrix $\mathbf{C}$) Q is very small, this channel estimator suffers from MUI in the same group, which causes large channel estimation error. To overcome this problem, we come up with a novel channel estimator. The system reserves some groups of subcarriers for channel estimation. We call these pilot groups, and the remainder, data groups. The pilot symbols of different users are time multiplexed and transmitted in different blocks of pilot groups. The receiver first obtains an instantaneous estimate of a user's CIR by using the pilot symbols, and then uses a linear interpolating filter to obtain the estimated CIR in different blocks. After the CIR is obtained, it can be translated to the frequency response on the subcarriers of the corresponding data group, which does not sacrifice optimality of MMSE or ML estimation [16]. If the receiver does not know the delay of a certain user, it needs at least $L+1$ subcarriers to estimate $L+1$ taps, although some of the taps are zero. After acquiring a user's timing, the receiver can use only $L_{s,\max}$ pilot subcarriers to estimate the channel. In the resulting channel estimation algorithm, we assume that the timing of a user has been acquired, and that the size of the pilot group is $Q \ge L_{s,\max}$.

Suppose that a user transmits a block of pilot symbols $\mathbf{s}_p$ every N_p blocks in the n_pth group, and assume that every pilot symbol has the same amplitude $|s_p|$. After OFDM demodulation, the received pilot signal vector in the kN_p block for the mth user in the nth group is given by

$$\begin{aligned}\mathbf{p}_{n,m}(kN_p) &= \mathcal{D}(\mathbf{s}_p)\bar{\mathbf{h}}_{n,m}^{(n_p)}(kN_p) + \mathbf{w}(kN_p) \\ &= \mathcal{D}(\mathbf{s}_p)\mathbf{F}_{n_p,m}\mathbf{h}_{n,m}(kN_p) + \mathbf{w}(kN_p) \quad (22)\end{aligned}$$

where $\bar{\mathbf{h}}_{n,m}^{(n_p)}(kN_p) := \mathbf{F}_{n_p,m}\mathbf{h}_{n,m}(kN_p)$ is the channel frequency response on the subcarriers in the pilot group. Based on the received signal (22), we use a least-squares error (LSE) approach to obtain an instantaneous estimate of $\mathbf{h}_{n,m}(kN_p)$. Since $\mathbf{F}_{n_p,m}^{\mathcal{H}}\mathbf{F}_{n_p,m} = Q\mathbf{I}_{L_{s,n,m}}$, the LSE estimate of $\mathbf{h}_{n,m}(kN_p)$ is written as [13, p. 229]

$$\hat{\mathbf{h}}_{n,m}(kN_p) = \mathbf{h}_{n,m}(kN_p) + \frac{\mathbf{F}_{n_p,m}^{\mathcal{H}}\mathcal{D}^{\mathcal{H}}(\mathbf{s}_p)\mathbf{w}(kN_p)}{Q|s_p|^2}. \quad (23)$$

Supposing that K instantaneous channel estimates $\hat{\mathbf{H}}_{n,m}(k) := [\hat{\mathbf{h}}_{n,m}((k-K+1)N_p), \ldots, \hat{\mathbf{h}}_{n,m}(kN_p)]^T$ are available, the CIR in block i, where $i = (k-1)N_p, \ldots, kN_p - 1$, can be obtained by filtering $\hat{\mathbf{H}}_{n,m}(k)$ to obtain $\hat{\hat{\mathbf{h}}}_{n,m}(i) = \mathbf{g}_i^{\mathcal{H}}\hat{\mathbf{H}}_{n,m}(k)$, where the linear filter $\mathbf{g}_i$ can be a simple truncated lowpass filter with the maximum Doppler frequency as its cutoff frequency, or a linear MMSE filter if the autocorrelation function of the CIR is available [2], [14]. Note that in the above interpolation, we have a delay of N_p blocks. If extra delay can be tolerated, we can improve our channel estimates by using more instantaneous channel estimates. Finally, the estimated channel frequency response on the subcarriers in the data group is given by $\hat{\hat{\mathbf{h}}}_{n,m}(i) = \mathbf{F}_{n,m}\hat{\hat{\mathbf{h}}}_{n,m}(i)$.

Because users share pilot groups, the bandwidth efficiency is the same as when pilot symbols are multiplexed with data symbols. However, the performance of the channel estimator is considerably improved since there is no interference with pilot symbols.

V. Simulations

In this section, we test GO-MC-CDMA via computer simulations. In our simulation, the orders of different users' channels are all chosen equal to $L_s = 3$; the different taps of each multipath channel are independently generated with an exponential power delay profile, i.e., the variance of the lth tap is $\sigma_l^2 = \exp(-l/L_s)/\sum_{l=0}^{L_s-1}\sigma_l^2, l = 0, \ldots, L_s - 1$. Quaternary phase-shift keying (QPSK) modulation is adopted; and the bit energy is defined as $\mathcal{E}_b = E(|s|^2)/2$. We set $M = 64$ subcarriers per block, and $Q = 4$ subcarriers per group. So, the maximum number of active users in each group is $N_a = 4$. We use Walsh-Hadamard spreading codes, and employ ML detection per group. When there are $N_a > 1$ active users in a group, we assume that all users $m = 1, \ldots, N_a - 1$ have the same power, while the user 0 of interest may have different power. We define the near–far ratio ν_f as $\nu_f = P_m/P_0, m > 0$, where P_m denotes the power for user m.

Performance comparison (MC-CDMA, GMC-CDMA, and GO-MC-CDMA): In MC-CDMA, the processing gain is set equal to the number of subcarriers $M = 64$, and the MMSE detector is employed. GMC-CDMA is simulated with a fixed block length and load adaptation [3]. In this setup, the maximum allowable number of users is eight, and each user transmits $K = 8$ symbols per block. Since the delay spread is $L_s = 3$, each user should use at least $J = 11$ subcarriers to guarantee symbol detectability (maximum diversity), according to [3]. Hence, the number of subcarriers is chosen to be $M = 88$. When the number of active users M_a changes, each active user is allocated $J = \lfloor M/M_a \rfloor$ subcarriers. The MMSE detector is employed because the ML detector has high complexity to jointly detect eight symbols per user. Fig. 5 shows BER versus load for these three systems, where the load is defined as the number of active users divided by the maximum number of users. For comparison, the single-user theoretical BER curve with the same channel power delay profile is also displayed. We see that the BER of GO-MC-CDMA is very close to the single-user bound, while the performance of both MC-CDMA and GMC-CDMA degrades as the load increases.

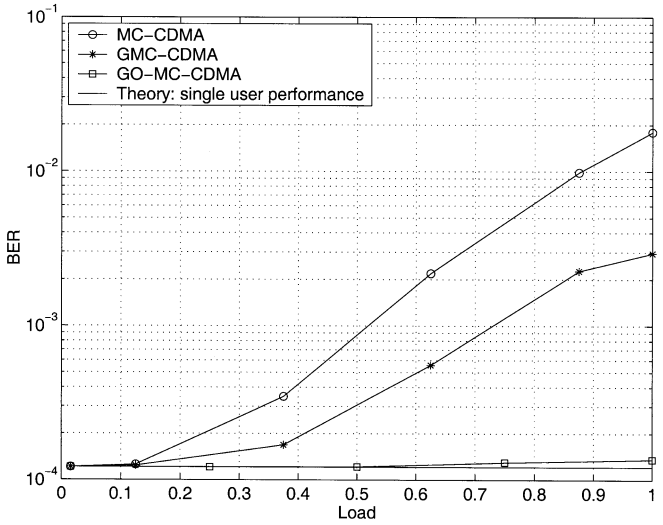

Fig. 5. BER of MC-CDMA, GMC-CDMA, and GO-MC-CDMA with perfect CSI, $\mathcal{E}_b/N_0 = 16$ dB, $\nu_f = 0$ dB.

GO-MC-CDMA with perfect CSI: Fig. 6(a) depicts the BER of GO-MC-CDMA with $\nu_f = 0$ dB. We see that when $N_a = 2$, the BER almost coincides with the single-user bound across the $\mathcal{E}_b/N_0$ region. When $N_a = 4$, BER reaches the single-user bound when $\mathcal{E}_b/N_0$ is high. The union bound in (17) and the bound on single-error PEP $P_1(e)$ are also shown in Fig. 6(a) for $N_a = 4$. It is observed that the union bound is very close to $P_1(e)$ at moderately high SNR, which confirms that the overall BER is dominated by the single-error probability, as we established through performance analysis in Section III. Note that $N_a = 2$ corresponds to a 27%–50% load, while $N_a = 4$ corresponds to a 77%–100% load. Fig. 6(b) depicts the BER of GO-MC-CDMA with $\nu_f = 3$ dB. The horizontal axis is the $\mathcal{E}_b/N_0$ of the weakest user 0. From Fig. 6(b), we deduce that the weak user's BER performance does not degrade by the strong interference of other users, which verifies our performance analysis in Section III. The union bound on SER again reaches $P_1(e)$ at high SNR.

GO-MC-CDMA with estimated CSI: In this example, the channel is estimated using the scheme developed in Section IV. Each active user transmits a block of pilot symbols in the pilot

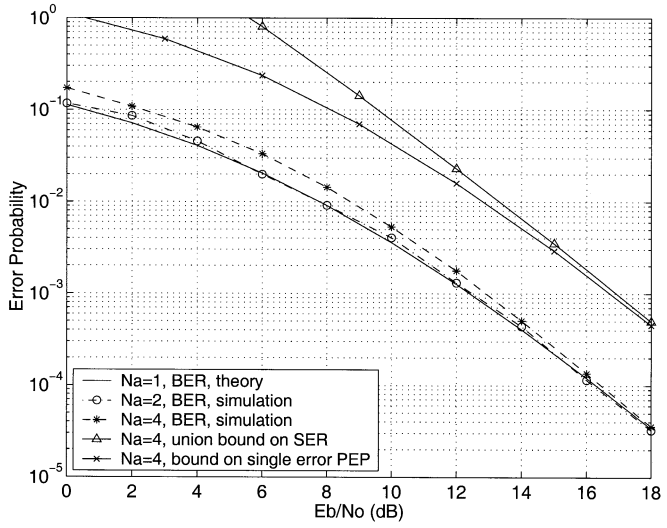

(a)

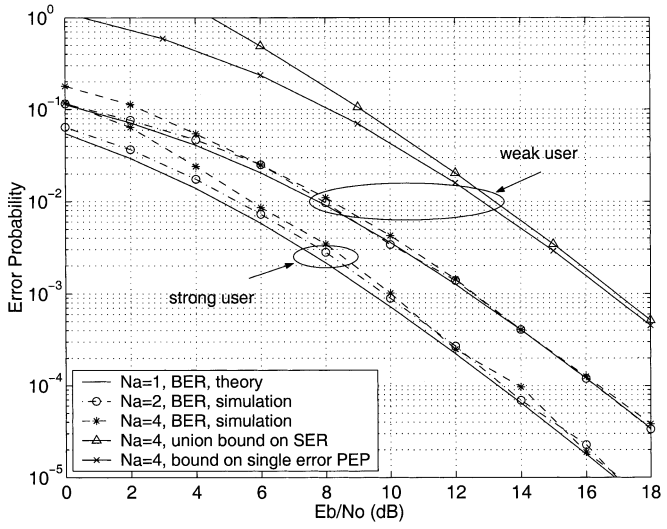

(b)

Fig. 6. BER versus $\mathcal{E}_b/N_0$ with perfect CSI. (a) $\nu_f = 0$ dB. (b) $\nu_f = 3$ dB.

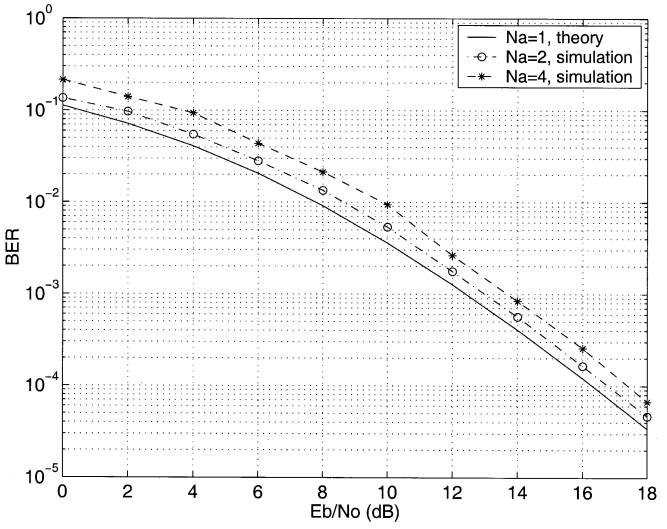

(a)

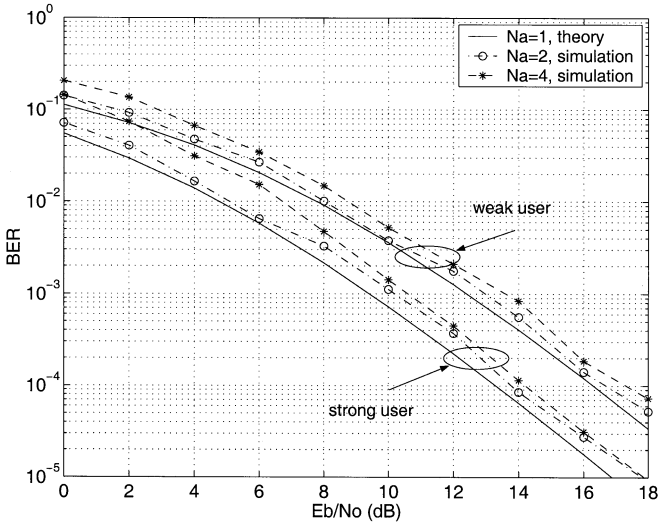

(b)

Fig. 7. BER versus $\mathcal{E}_b/N_0$ with estimated CSI, and $\nu = 10$ km/h. (a)$\nu_f = 0$ dB. (b)$\nu_f = 3$ dB.

group every $N_p = 9$ blocks. This corresponds to slot format 12 of dedicated downlink physical channel in Third–Generation Partnership Project (3GPP) wideband CDMA (WCDMA) [17], which has data rate 120 kb/s. The carrier frequency is 2 GHz; the symbol rate is 60 ks/s, and thus the duration of every block (with CP) is 17.4 μs. A seven-tap MMSE interpolating filter is used in channel estimation [2]. Fig. 7(a) and (b) show BER for $\nu_f = 0$ dB and $\nu_f = 3$ dB, when the velocity of the mobile is 10 km/h. Comparing Fig. 7(a) and (b) with Fig. 6(a) and (b), we see that when $N_a = 2$, the BER degradation caused by channel estimation is very small. When $N_a = 4$, BER performance using estimated channels is about 0.5 dB worse than that using the true channel at BER $= 10^{-4}$. Comparing Fig. 7(a) with Fig. 7(b), we observe again that a high near–far ratio does not degrade the performance of the weak user. When the mobile velocity is 100 km/h, BER curves are depicted in Fig. 8(a) and (b) for $\nu_f = 0$ dB and $\nu_f = 3$ dB, respectively. We see that the BERs exhibit larger degradation because the channel estimation error is larger. The largest performance degradation at BER $= 10^{-4}$ is about 2 dB when $N_a = 4$, and $\nu_f = 3$ dB.

VI. Conclusions

We developed a group orthogonal MC-CDMA system with affordable receiver complexity. We showed that the performance of GO-MC-CDMA comes very close to the single-user performance even when the system is fully loaded. The superior performance of GO-MC-CDMA is achieved by transmitting signals of a small group of users on a set of judiciously selected subcarriers, which enables maximum diversity per user. MUI among the users in the same group is suppressed via MUD, which becomes practically feasible because we select groups of small size. A channel estimator resilient to MUI is also developed. Performance degradation with estimated channels is confirmed to be small. In short, GO-MC-CDMA is a practically feasible system with a number of attractive features.[1]

[1]The views and conclusions contained in this document are those of the authors and should not be interpreted as representing the official policies, either expressed or implied, of the Army Research Laboratory or the U. S. Government.

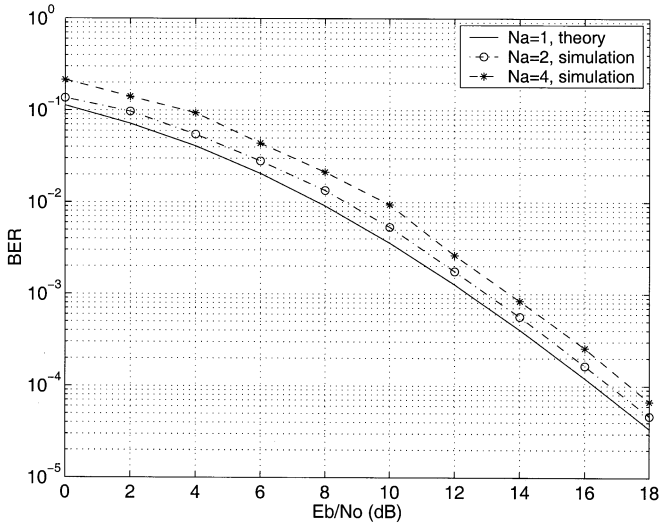

(a)

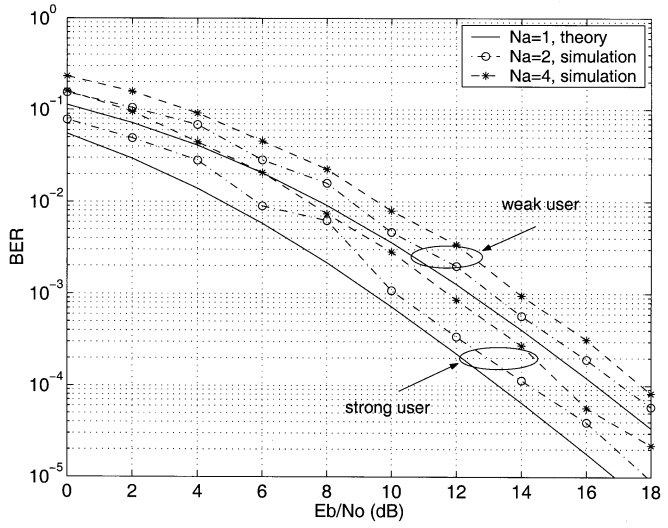

(b)

Fig. 8. BER versus $\mathcal{E}_b/N_0$ with estimated CSI, and $\nu = 100$ km/h. (a) $\nu_f = 0$ dB. (b) $\nu_f = 3$ dB.

ACKNOWLEDGMENT

The authors would like to thank the anonymous reviewers for their careful reading and critique of the manuscript. Their comments and suggestions improved the presentation of this paper.

REFERENCES

[1] J. Boutros and E. Viterbo, "Signal space diversity: a power- and bandwidth-efficient diversity technique for the Rayleigh fading channel," *IEEE Trans. Inform. Theory*, vol. 44, pp. 1453–1467, July 1998.

[2] J. K. Cavers, "An analysis of pilot-symbol-assisted modulation for Rayleigh fading channels," *IEEE Trans. Veh. Technol.*, vol. 40, pp. 686–693, Nov. 1991.

[3] G. B. Giannakis, A. Stamoulis, Z. Wang, and P. Anghel, "Load-adaptive MUI/ISI-resilient generalized multi-carrier with DF receivers and blind estimation capabilities," *Eur. Trans. Telecommun.*, vol. 11, pp. 527–537, Nov./Dec. 2000.

[4] G. B. Giannakis, Z. Wang, A. Scaglione, and S. Barbarossa, "AMOUR—generalized multicarrier transceivers for blind CDMA regardless of multipath," *IEEE Trans. Commun.*, vol. 48, pp. 2064–2076, Dec. 2000.

[5] D. L. Goeckel and W. E. Stark, "Optimal diversity allocation in multiuser communication systems—Part I: System model," *IEEE Trans. Commun.*, vol. 47, pp. 1828–1836, Dec. 1999.

[6] ——, "Optimal diversity allocation in multiuser communication systems—Part II: Optimization," *IEEE Trans. Commun.*, vol. 48, pp. 45–52, Jan. 2000.

[7] D. L. Goeckel and G. Ananthaswamy, "On the design of multidimensional signal sets for OFDM systems," *IEEE Trans. Commun.*, vol. 50, pp. 442–452, Mar. 2002.

[8] G. H. Golub and C. F. V. Loan, *Matrix Computations*. Baltimore, MD: Johns Hopkins Univ. Press, 1996.

[9] S. Hara and R. Prasad, "Overview of multicarrier CDMA," *IEEE Commun. Mag.*, pp. 126–133, Dec. 1997.

[10] ——, "Design and performance of multicarrier CDMA system in frequency-selective Rayleigh fading channels," *IEEE Trans. Veh. Technol.*, vol. 48, pp. 1584–1594, Sept. 1999.

[11] R. A. Horn and C. R. Johnson, *Matrix Analysis*. Cambridge, U. K.: Cambridge Univ. Press, 1985.

[12] A. Høst-Madsen and X. Wang, "Performance of blind and group-blind multiuser detectors," *IEEE Trans. Inform. Theory*, vol. 48, pp. 1849–1872, July 2002.

[13] S. T. Kay, *Fundamentals of Statistical Signal Processing, Volume I: Estimation Theory*. Englewood Cliffs, NJ: Prentice-Hall, 1993.

[14] F. Ling, "Optimal reception , performance bound, and cutoff rate analysis of references-assisted coherent CDMA communications with applications," *IEEE Trans. Commun.*, vol. 47, pp. 1583–1591, Oct. 1999.

[15] Z. Liu, Y. Xin, and G. B. Giannakis, "Linear constellation precoding for OFDM with maximum multipath diversity and coding gains," *IEEE Trans. Commun.*, vol. 51, pp. 416–427, Mar. 2003.

[16] M. Morelli and U. Mengali, "A comparison of pilot-aided channel estimation methods for OFDM systems," *IEEE Trans. Signal Processing*, vol. 49, pp. 3065–3073, Dec. 2001.

[17] Physical Channels and Mapping of Transport Channels, 3GPP Tech. Spec. TS 25.211, 2001.

[18] J. G. Proakis, *Digital Communications*. New York: McGraw-Hill, 1995.

[19] T. S. Rappaport, *Wireless Communications*. Englewood Cliffs, NJ: Prentice-Hall, 1996.

[20] H. Sari and G. Karam, "Orthogonal frequency-division multiple access and its applications to CATV network," *Eur. Trans. Telecommun.*, pp. 507–516, Nov./Dec. 1998.

[21] M. Schwartz, W. R. Benett, and S. Stein, *Communication Systems and Techniques*. New York: IEEE Press, 1996.

[22] M. K. Varanasi, "Parallel group detection for synchronous CDMA communications over frequency-selective Rayleigh fading channels," *IEEE Trans. Inform. Theory*, vol. 42, pp. 116–128, Jan. 1996.

[23] S. Verdú, *Multiuser Detection*. Cambridge, U. K.: Cambridge Univ. Press, 1998.

[24] E. Viterbo and J. Boutros, "A universal lattice code decoder for fading channel," *IEEE Trans. Inform. Theory*, vol. 45, pp. 1639–1642, July 1999.

[25] Z. Wang and G. B. Giannakis, "Wireless multicarrier communications: where Fourier meets Shannon," *IEEE Signal Processing Mag.*, vol. 47, pp. 29–48, May 2000.

[26] ——, "Block precoding for MUI/ISI-resilient generalized multicarrier CDMA with multirate capabilities," *IEEE Trans. Commun.*, vol. 49, pp. 2016–2027, Nov. 2001.

[27] Z. Wang, S. Zhou, and G. B. Giannakis, "Joint coded-precoded OFDM with low-complexity turbo decoding," in *Proc. European Wireless Conf.*, Florence, Italy, Feb. 25–28, 2002, pp. 648–654.

[28] Z. Wang and G. B. Giannakis, "Complex-field coding for OFDM over fading wireless channels," *IEEE Trans. Inform. Theory*, vol. 49, pp. 707–720, Mar. 2003.

[29] P. Xia, S. Zhou, and G. B. Giannakis, "Bandwidth- and power-efficient multicarrier multiple access," *IEEE Trans. Commun.*, vol. 51, pp. 1828–1837, Nov. 2003.

[30] Y. Xin, Z. Wang, and G. B. Giannakis, "Space–time diversity systems based on linear constellation precoding," *IEEE Trans. Wireless Commun.*, vol. 2, pp. 294–309, Mar. 2003.

[31] S. Zhou, G. B. Giannakis, and A. Swami, "Frequency-hopped generalized MC-CDMA for multipath and interference suppression," in *Proc. MILCOM Conf.*, Anaheim, CA, Oct. 2000, pp. 937–942.

Xiaodong Cai (M'01) received the B.S. degree from Zhejiang University, Hangzhou, China, the M.Eng. degree from the National University of Singapore, Singapore, and the Ph.D. degree from the New Jersey Institute of Technology, Newark, in 2001, all in electrical engineering.

From February 2001 to June 2001, he was a Member of Technical Staff at Lucent Technologies, NJ, working on a WCDMA project; from July 2001 to October 2001, he was a Senior System Engineer at Sony Technology Center, San Diego, CA, involved in developing high-data-rate wireless modems. Since November 2001, he has been a Postdoctoral Research Associate in the Department of Electrical and Computer Engineering, University of Minnesota, Minneapolis. His research interests lie in the areas of communication theory, signal processing, and wireless networks.

Shengli Zhou (M'03) received the B.S. degree in 1995 and the M.Sc. degree in 1998, from the University of Science and Technology of China (USTC), Hefei, China, both in electrical engineering and information science. He received the Ph.D. degree in electrical engineering from the University of Minnesota, Minneapolis, in 2002.

He joined the Department of Electrical and Computer Engineering, University of Connecticut, Storrs, as an Assistant Professor in 2003. His research interests lie in the areas of communications and signal processing, including channel estimation and equalization, multiuser and multicarrier communications, space–time coding, adaptive modulation, and cross-layer designs.

Georgios B. Giannakis (S'84–M'86–SM'91–F'97) received the Diploma in electrical engineering from the National Technical University of Athens, Greece, in 1981. He received the MSc. degree in electrical engineering in 1983, M.Sc. degree in mathematics in 1986, and the Ph.D. degree in electrical engineering in 1986, from the University of Southern California (USC), Los Angeles.

His general interests span the areas of communications and signal processing, estimation and detection theory, time-series analysis, and system identification, subjects on which he has published more than 180 journal papers, 300 conference papers, and two edited books. Current research focuses on transmitter and receiver diversity techniques for single- and multiuser fading communication channels, comples-field and space–time coding, multicarrier, ultra-wideband wireless communication systems, cross-layer designs, and distributed sensor networks.

Dr. Giannakis is the corecipient of four Best Paper Awards from the IEEE Signal Processing (SP) Society (1992, 1998, 2000, and 2001). He also received the Society's Technical Achievement Award in 2000. He co-organized three IEEE-SP Workshops, and guest co-edited four special issues. He has served as Editor in Chief for the IEEE SIGNAL PROCESSING LETTERS, as Associate Editor for the IEEE TRANSACTIONS ON SIGNAL PROCESSING and the IEEE SIGNAL PROCESSING LETTERS, as secretary of the SP Conference Board, as member of the SP Publications Board, as member and vice-chair of the Statistical Signal and Array Processing Technical Committee, and as chair of the SP for Communications Technical Committee. He is a member of the Editorial Board for the PROCEEDINGS OF THE IEEE, and the steering committee of the IEEE TRANSACTIONS ON WIRELESS COMMUNICATIONS. He is a member of the IEEE Fellows Election Committee, and the IEEE-SP Society's Board of Governors.